Synthesis and characterization of β-MnO_2 nanoparticles for hydrogen production

J. Sathya[a,*], S. Kanmani[b]
[a]*Research Scholar, Centre for Environmental Studies, Anna University, Chennai – 600 025, Tamilnadu, India*
[b]*Director and Professor, Centre for Environmental Studies, Anna University, Chennai – 600 025, Tamilnadu, India*

The nanoparticles were hydrothermally synthesized using β-MnO_2 nanoparticles were primed using a chemical reduction method. β-MnO_2 nanoparticles were validated to occur in the type of nanocrystals with a high specific surface area of 109 m^2/g. While β-MnO_2 nanoparticles were used as a photocatalyst for wastewater treatment, they demonstrated vastly more efficient hydrogen production action. The greater hydrogen production evaluate (750 mol^{-1}/h) was attained by separating the artificial sulphide effluent (0.2 M) using β-MnO_2 NPs in a photocatalytic reaction. The findings demonstrate the β-MnO2 NPs' efficient power abilities, notably for photocatalytic hydrogen detachment from sulphide wastewater. From this investigation, we evidenced a recyclable tactic for impactful sewage treatment through the use of photocatalytic water splitting employing β-MnO_2 NPs.

(Received November 22, 2021; Accepted February 28, 2022)

Keywords: H_2 production, TEM, β-MnO_2 NPs, Reduction method

1. Introduction

Hydrogen energy, a new-type clean energy carrier [1], has attracted much attention to solve the increasingly urgent energy and environment problems. Therefore, much research has been carried out on hydrogen production technique [2]. Among different hydrogen production routes, the photocatalytic water-splitting is a promising technology for hydrogen generation by utilizing abundant solar light. It has been extensively studied by many research groups in recent years [3]. The key to improving photocatalytic hydrogen production technique is the preparation of highly efficient and stable photocatalysts. Conventional photocatalysts were almost exclusively focused on the study of semiconductor materials since TiO_2 electrode was found to be able to achieve water-splitting as photocatalyst in 1972 [4]. However, in order to enhance the photocatalytic activity, noble metal nanoparticles incorporated in semiconductor, namely plasmonic photocatalyst, has been successfully applied [5]. Besides, the mechanism of plasmonic photocatalysis was firstly proposed by Koichi Awazu in 2008 [6]. The metallic plasmonic nanoparticles have an excellent mobility of charge carriers a high absorption, and they also have the ability to tune the resonance wavelength by changing their size or shape, so it is promsing that the entire solar spectrum can be exploited [7]. But since Essentially MnO_2 nanoparticles are versatile material in both technical and bright features considered to other metal oxides. For instance, MnO_2 NCs has also shown potential in a broad array of applications, including catalysis, molecular adsorption, sensors, energy storage electrodes, and so on [8].Furthermore, MnO_2 nanoparticles could be used in technological innovation like dye degradation [9]wastewater treatment [10] photo catalytic degradation of organic pollutants [11]and photo-electrochemical hydrogen production [12]. The aim of the present exploit, facile method of β-MnO_2 nanoparticles were fabricated by hydrothermal approach, the obtained nanoparticles were evidenced by analytical characterization and mainly focused for hydrogen production from synthetic waste water were discussed.

* Corresponding author: sathyaj.study@gmail.com
https://doi.org/10.15251/JOR.2022.181.93

2. Experimental details

All required materials, such as $KMnO_4$ (99.9%) and $NaBH_4$ (99.9%), were procured from Sigma Pvt. Ltd., India and then used exactly as acquired. Milli-Q water has been used in the commissioning and soaking process.

2.1. Preparation of β-MnO_2 Nanoparticles

The process for making β-MnO_2, excluding injecting 2 mL of 0.1M $NaBH_4$ solution. A and 15 mL MQ water was added to make 50 mL. The brown residue was then strained, soaked in water and ethanol, and dried in oven for 24 hours at 80 degrees Celsius. The material was sintered after 3 hours at 400 degrees Celsius, attaining -MnO_2 as a blackened residue [13].

2.2. Evaluation of photo catalytic hydrogen production

The testing was performed out in a 250 ml photo catalytic reactor that was exposed with a light source. There seem to be two tubes on the reactor. Even though illustrated in the diagram, one inlet was used to expel nitrogen (N_2) gas while the other tube was employed to harvest Hydrogen ions using an upward displacing container. Prior to the actual process, nitrogen was evacuated through the inlet to exclude oxygen. The illuminating being furnished with 120 W mercury lamps. A peristaltic compressor was used to disperse and various 5, 10, 15, 20 and 25mg of photo catalyst in a 100 ml aqueous solution containing 0.2 M Na_2S and 0.25 M Na_2SO_3. The photo reactor was operated at ambient temperature. H_2 production was measured employing GC over being captured in a water displacement container (Shimadzu 14B, Molecular sieve -5 A column, TCD detector and N_2 carrier gas) [14].

3. Results and discussion

3.1. XRD Structural analysis for Analysis of crystalline phase

Xrd pattern of β-MnO_2 organized with 2 mL of SB solution. seem to at 28.8, 37.4, 43.0, 56.9 and 72.6, which were attributed to crystalline phase of (110), (101), (111), (220), and (301) MnO_2 in the tetragonal crystal with P42/mnm space group and quite well archived by β-MnO_2 (JCPDS Card No: 024-073) [15]. Moreover, the mean crystallite size of the prepared MnO_2 was assessed using the Scherer formula (1),

$$Dp = (K\ k) / (b\ Cosh) \quad (1)$$

where 'K' is the shape factor, 'k' is the X-ray wavelength, 'b' is the full wave half maximum (FWHM) of the XRD peak, and 'h' is the Braggs angle. The mean crystallite size of -MnO_2 was found to be around 6 nm, respectively. The XRD pattern of β-MnO_2 shows a tetragonal rutile structure with an I_4/m space group [16, 17].

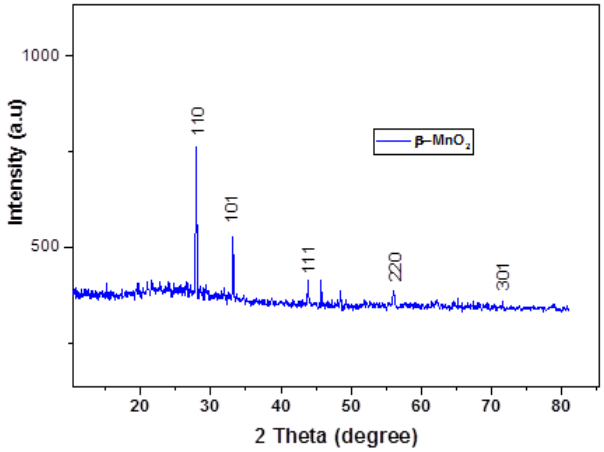

Fig. 1. XRD pattern of β-MnO_2 nanoparticles by hydrothermal approach.

3.2. SEM analysis

Figure 2 (a) shows HRSEM images of MnO_2 NPs, confirming that the size of all synthesized products is non-uniform. As a consequence, it could be the combined effect of spherical morphology particles and the formation of non-equal crystalline phase during the prediction phase.

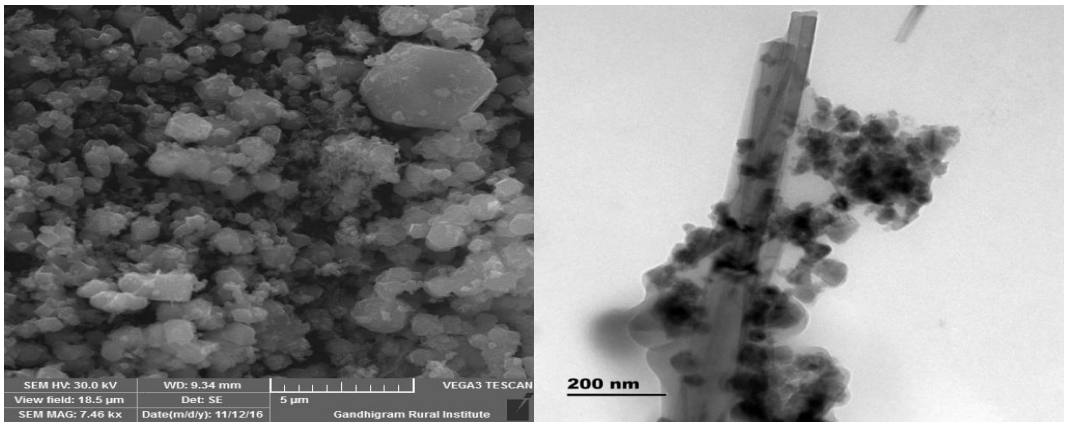

(a) *(b)*

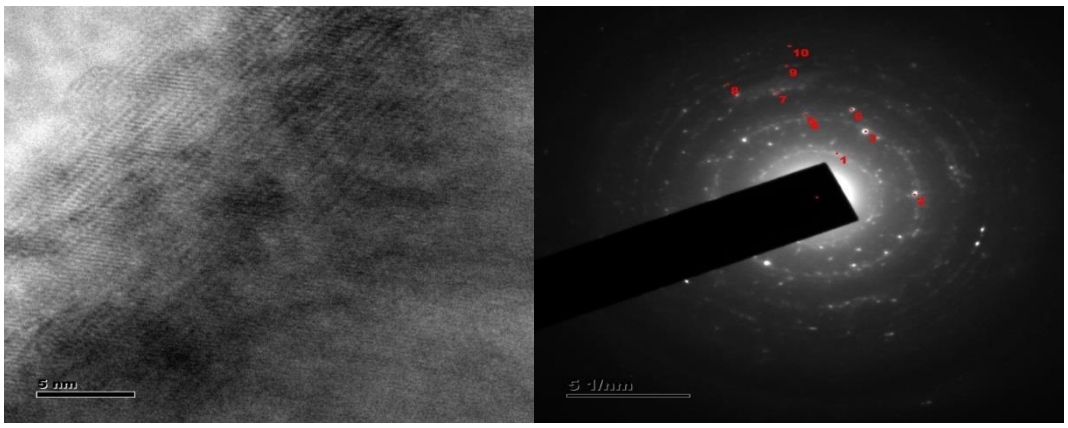

(c) *(d)*

Fig. 2. (a) SEM – Micrograph (b) TEM Micrograph (c) HR-TEM photograph (d) SAED pattern.

Because of the low urea-to-precursor ratio of 1:1, the number of sodium boro-hydride around Mn-O in the solution was very limited. Because the small amount of sodium borohydride didn't supply adequate hydroxyl groups during the reaction, non-uniformly sized spherical like particles were formed, and the shape varied from spherical to rod-like morphological features after the equilibrium was reached. Previously, similar findings were observed for CeO_2–ZrO_2 nanocomposites [21]. We noted from the HRSEM images that the emergence of spherical nanoparticles-like structural system was caused by adhesion pursued by nanoparticle agglomeration. It was noteworthy that the particles were gathered together like an outcome of magnetic interplay among the droplets [22, 23].

3.3. TEM/HR-TEM investigation

HR-TEM statistics were used to describe the morphological characteristics and structural properties of -MnO2. Fig.4 (b&c) show the typical HR-TEM images. HR-TEM images show a nano-spherical arrangement with a diameter of 10–50 nm. Due to the obvious magnetic natural surroundings of the components, the occurring spherical morphology specimen are constructed by the modest aggregation of nanoparticles. The SAED template of pristine MnO_2, as seen in Fig. 4c, acknowledged that the specimens are quite well crystallized in essence

3.4. EDS analysis

Because the elemental composition of the electrode material is required for the hydrogen energy production application, the elemental and chemical compositions of MnO_2 NPs were assessed using EDX. The primed specimens' EDX spectra were examined in the binding area of 0–10 keV, as shown in Fig. 3. Figure 5 indicate the existence of stoichiometric proportions of O and Mn specimen, and it obviously proves the existence of Mn and O in -MnO_2 nanoparticles [13].

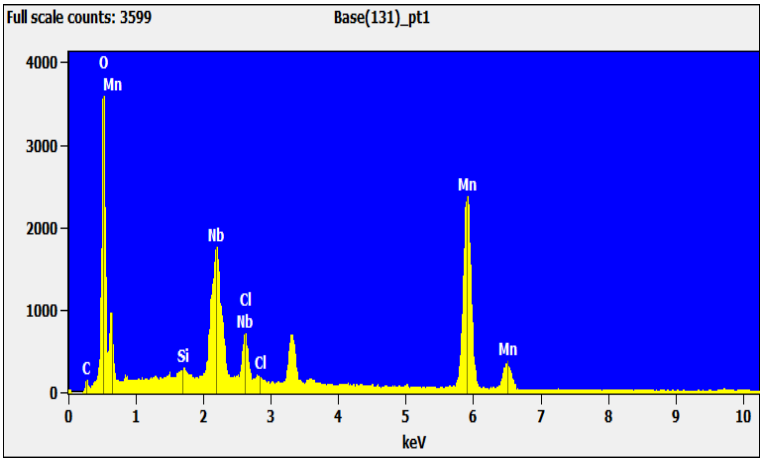

Fig. 3. Elemental composition spectrum of β-MnO_2 nanoparticles.

3.5. BET analysis

Figure 4a depicts the β-MnO_2 nanoparticles' N_2 adsorption–desorption isotherm curvatures. According to the BET assessment, the specific surface area (Ass) of β-MnO_2 was 64, 822, and 109m^2/g, respectively. The porosity features of β-MnO_2 are depicted in Figure 6b. Both specimens clearly exposed their pore sizes on a nanoscale dimensions; that is, the mean particle sizes of β-MnO_2 were predicted to be 8.78 and 7.66 nm, respectively. We also revealed that the β-MnO_2 nanoparticles have a larger overall pore volume (i.e., 0.0204 cm3/g) than the β-MnO_2 nanoparticles (i.e., 0.0141 cm^3/g) using BJH assessment. Furthermore, the β-MnO_2 has an average pore size of 2.8 nm and a total pore volume of 0.0459 cm^3/g. The increased pore volume of β-MnO_2 predicted to arise from the embedment of hierarchical porous β-MnO_2 nanoparticles with

mesoporous is successful in enhancing photocatalytic hydrogen production, as described in later [24].

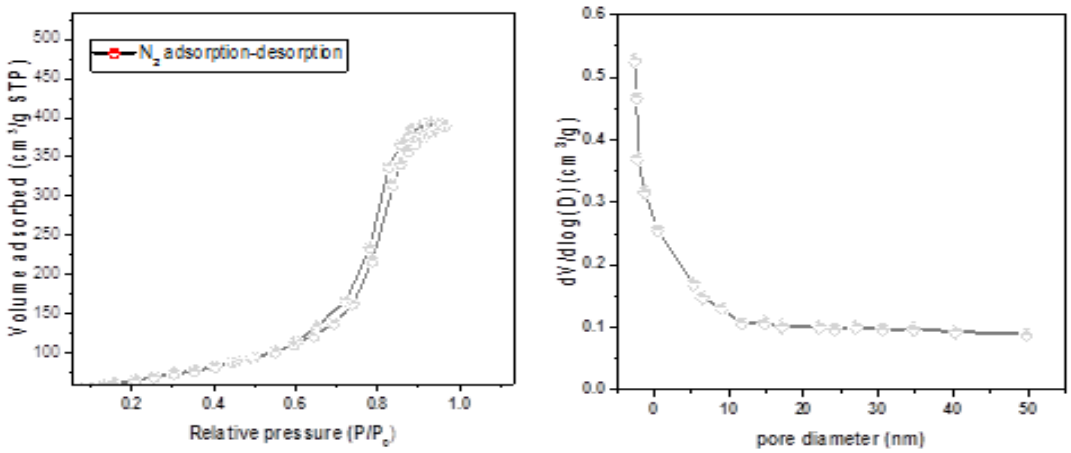

Fig. 4. (a) BET isotherm analysis of β-MnO_2 nanoparticles (b) pore volume vs pore diameter of β-MnO_2 nanoparticles.

3.6. Effect of drug loaded activity

By adjusting the catalyst dose in the range of 5,10,15,20 and 25mg, the influence of catalyst loading on the development of H_2 through synthetic sulphide effluent was examined. Sulfite ion concentration, sulphide ion concentration, and pH were sustained at 0.2 M, 0.25 M, 100 mL, 120 W, and 13 appropriately. Apparently hydrogen production has increased while the catalyst dosages was raised from 5, 10, 15, 20and 25mg. The existence of additional binding sites in the enhanced photocatalyst was the reason for this. Production of hydrogen improved as the dosage of photocatalyst was raised from (0.3 – 0.5) g. It inhibited the light absorption of the system provides intrinsic droplets [25] and even the concentration of colloidal matter, which had deleterious effect on scribing and screening processes can be seen in fig 5.

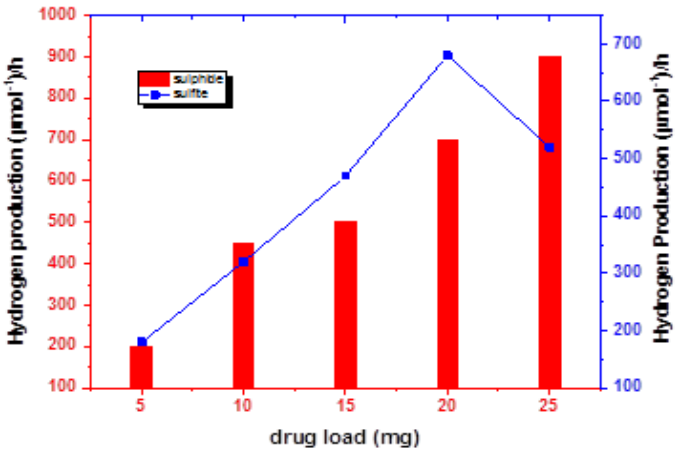

Fig. 5. Effect of catalyst dose on hydrogen production

3.7. Effect of pH on hydrogen production

Effect of pH calibration could perhaps being performed out and after sulfite, sulphide, and accelerator dose adjustment since it represents a crucial impact in the inherent nature of sulphur compounds. When the pH level rises from 4 to 13, hydrogen generation develops as well. Even as pH rises from 12 to 13, the amount of hydrogen in the solution decreases, as illustrated in fig.6.

This is caused to an increase in the dose of the OH- ion. Whenever the proportion of hydroxyl ion becomes too excessive, numerous photoinduced hydrogen atoms combine with hydroxyl ion, leading to the formation water [26, 27] Decreased hydrogen production is also attributed to photocatalyst destruction during greater alkaline medium.

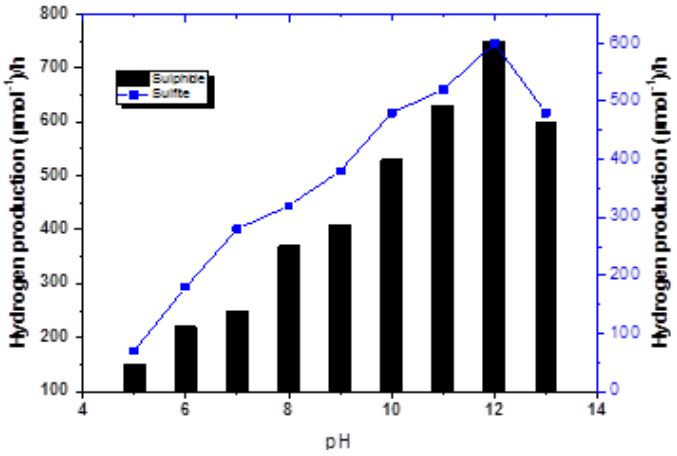

Fig. 6. Effect of pH on hydrogen production

4. Conclusions

The hydrothermal framework was used to fruitfully develop the β-MnO_2 NPs. XRD, SEM and TEM analyses revealed that the β -MnO_2 NPs were gathered. When the influence of pH was essential on the β-MnO_2 NPs as a photocatalytic carrier for artificial treating wastewater, an elevated hydrogen production capacity of 750 mol^{-1}/h has been attained for around 1 hour. We believed to be due the high conductivity and permeability of the β-MnO_2 NPs' awesome H_2 production process to rapid career advancement and an enormous amount of binding sites for chemical process. The findings suggest that the hydrothermal strategy to developing β-MnO_2 NPs was indeed a great resource for repurposing sewage treatment through hydrogen evolution.

References

[1] A. Midilli, M. Ay, I. Dincer, M.A. Rosen, Renewable and Sustainable Energy Reviews, 2005, 9, 255; https://doi.org/10.1016/j.rser.2004.05.003
[2] (a) K. J. Wu, J. S. Chang, Process biochemistry, 2007, 42, 279; https://doi.org/10.1016/j.procbio.2006.07.021; (b) M.M. Najafpour, G. Renger, M. Hołynska, A.N. Moghaddam, E.-M. Aro, R.Carpentier, H. Nishihara, J.J. Eaton-Rye, J.-R. Shen, S.I. Allakhverdiev, Chem.Rev, 2016, 116, 2886; https://doi.org/10.1021/acs.chemrev.5b00340; (c) J. Liu, Y. Liu, N.Y. Liu, Y.Z. Han, X. Zhang, H. Huang, Y. Lifshitz, S.-T. Lee, J.Zhong and Z.K. Kang, Science, 2015, 347, 970; https://doi.org/10.1126/science.aaa3145
[3] (a) A. Kudo; Y. Miseki, Chem. Soc. Rev., 2009, 38, 253; https://doi.org/10.1039/B800489G; (b) K. Sivula, F. L. Formal; M. Gratzel, ChemSusChem, 2011, 4, 432; https://doi.org/10.1002/cssc.201000416; (c) T. Hisatomi, J. Kubota, K. Domen, Chem. Soc. Rev., 2014, 43, 7520; https://doi.org/10.1039/C3CS60378D; (d) S. Martha, P. C. Sahooa, K. M. Parida, RSC Adv., 2015, 5, 61535. (e)Y. K. Wei, J. Z. Su, X. K. Wan, L. J. Guo and L. Vayssieres, Nano Research, 2016, 9, 1561; https://doi.org/10.1039/C5RA11682A
[4] A. Fujishima; K. Honda, Nature, 1972, 238, 37; https://doi.org/10.1038/238037a0
[5] (a) S. F. Kou, W. Ye, X.Guo, X. F.Xu, H. Y.Sun, J.Yang, RSC Advances, 2016, 6, 39144; https://doi.org/10.1039/C6RA04444A; (b) X. M. Hou, Mater Lett. 2015, 139, 201; https://doi.org/10.1016/j.matlet.2014.10.053; (c) Y. K. Li, H. M. Yu, C. K. Zhang, L. Fu, G. F. Li,

Z. G. Shao, B.L.Yi, Int J Hydrogen Energ, 2013, 38, 13023; https://doi.org/10.1016/j.ijhydene.2013.03.122; (d) J. J. Wu, S. L. Lu, D. H. Ge, L. Z. Zhang, W. Chen H. W. Gu. RSC Adv., 2016,6, 67502; https://doi.org/10.1039/C6RA10408H
[6] K. Awazu, M. Fujimaki, C. Rockstuhl, J. Tominaga, H. Murakami, Y. Ohki, N. Yoshida, T. Watanabe, J Am Chem Soc, 2008, 130, 1676; https://doi.org/10.1021/ja076503n
[7] Djurišic, A.B.; Leung, Y.H.; Ching Ng, A.M., Mater. Horiz. 2014, 1, 400-410; https://doi.org/10.1039/c4mh00031e
[8] Debnath, B.; Roy, A.S.; Kapri, S.; Bhattacharyya, S., Chemistry Select 2016, 1, 4265-4273; https://doi.org/10.1002/slct.201600806
[9] Primo, A., Marino, T., Corma, A., Molinari, R. & García., J. Am. Chem. Soc. 2011, 133, 6930-6933; https://doi.org/10.1021/ja2011498
[10] Wang, R.; Hao, Q.; Feng, J.;Wang, G.-C.; Ding, H.; Chen, D.; Ni, B. J. Alloys Compd. 2019, 786, 418-427; https://doi.org/10.1016/j.jallcom.2019.02.009
[11] Ding, Y.;Wei, D.; He, R.; Yuan, R.; Xie, T.; Li, Z., Appl. Catal. B 2019, 258, 117948; https://doi.org/10.1016/j.apcatb.2019.117948
[13] Veeman Sannasi, Karuppuchamy Subbian, J Mater Sci: Mater Electron 2020, https://link.springer.com/article/10.1007/s10854-020-04272-z
[14] Thangam N, Suganya Devi B, Lalitha Muthu AC, International Journal of New Technology and Research (IJNTR) ISSN: 2454-4116, Volume-1, Issue-1, May 2015 Pages 04-10
[15] H. Wang, X. Fan, X. Zhang, Y. Huang, Q. Wu, Q. Pan, Q. Li, RSC Adv. 7, 23328 (2017) https://doi.org/10.1039/C7RA02932B
[16] Y. Zhang, C. Sun, P. Lu, S. Song, D. Xue, CrysEngComm. 14, 5892-5897 (2012); https://doi.org/10.1039/c2ce25610j
[17] K. Chen, Y.D. Noh, K. Li, S. Komarneni, D. Xue, J. Phys. Chem. C 117, 10770-10779 (2013); https://doi.org/10.1021/jp4018025
[18] K.M. Racik, K. Guruprasad, M. Mahendran, J. Madhavan, T. Maiyalagan, M.V. Anton Raj,. J. Mater. Sci. 30, 5222-5232 (2019); https://doi.org/10.1007/s10854-019-00821-3
[19] M. Ma, Y. Zhang, W. Yu, H.Y. Shen, H.Q. Zhang, N. Gu, Colloids Surf. A 212, 219 (2003) https://doi.org/10.1016/S0927-7757(02)00305-9
[20] C. Julien, M. Massot, R. Baddour-Hadjean, S. Franger, S. Bach, J.P. Pereira-Ramos, Solid State Ionics 159, 345-356 (2003); https://doi.org/10.1016/S0167-2738(03)00035-3
[21] X. Zhang, Q. Wang, J. Zhang, J. Wang, M. Guo, S. Chen, C. Li, C. Hu, Y. Xie, RSC Adv. 5, 89976-89984 (2015); https://doi.org/10.1039/C5RA19271D
[22] M.M.L. Sonia, S. Anand, V.M. Vinosel, M.A. Janifer, S. Pauline, J. Mater. Sci. Mater. Electron. 29(17), 15006-15021 (2018); https://doi.org/10.1007/s10854-018-9639-2
[23] A.P. Amaliya, S. Anand, S. Pauline, J. Magn. Magn. Mater. 467, 14-28 (2018) https://doi.org/10.1016/j.jmmm.2018.07.058
[24] Sekar, S.; Lee, Y.; Kim, D.Y.; Lee, S., Nanomaterials 2019, 9, 871; https://doi.org/10.3390/nano9060871
[25] Preethi, V., Kanmani, S., International Journal of Hydrogen Energy, (2014), 39, 1612-1622 https://doi.org/10.1016/j.ijhydene.2013.11.029
[26] Strataki, N, Antoniadou, M, Dracopoulos, V., Lianos, P., Catalyst Today, (2010) 151, 53-57 https://doi.org/10.1016/j.cattod.2010.03.036
[27] Bao, N.Z., Shen, L.M., Takata, T., Domen, K., Chemistry Material, (2008), 20, 110-117 https://doi.org/10.1021/cm7029344